# k0-IPEN: a new software for INAA

**Mauro Da Silva Dias**[1] **· Renato Semmler**[1] **· Marina Fallone Koskinas**[1] **· Denise Simões Moreira**[1] **· Ione Makiko Yamazaki**[1] **· Franco Brancaccio**[1] **· Lívia Fernandes Barros**[1] **· Rafael Vanhoz Ribeiro**[1] **· Thales Salvador Lima de Morais**[1]

## Abstract

A software package for INAA (Instrumental Neutron Activation Analysis), developed at the Nuclear Metrology Laboratory of the IPEN-CNEN/SP, called k0-IPEN, is described. The package consists of a main program linked to nine subprograms designed to perform automatically most of the tasks necessary in order to obtain the mass fractions of the irradiated samples. External efficiency curves calculated by the Monte Carlo code MCNP6 can be read to extend the calibration curve to source to detector distances where only a few experimental points are available. Covariance analysis was used in all steps of the calculation. The validation of the code was tested in an intercomparison sponsored by the IAEA.

**Keywords** Neutron activation analysis · k0-Method · Software intercomparison · Neutron flux parameters · Germanium detector · Monte Carlo

## Introduction

The Nuclear Metrology Laboratory (Laboratório de Metrologia Nuclear—LMN) at the IPEN-CNEN/SP (Nuclear and Energy Research Institute, National Nuclear Energy Commission) in São Paulo, Brazil, does research in two interrelated areas, namely: Radionuclide Metrology and Neutron Metrology. In the latter area, the LMN has published papers on the measurement of neutron cross sections [e.g., 1, 2] and $k_0$ parameters [e.g., 3, 4]. These results are obtained by running several codes, which perform individual tasks such as: determination of spectrum net peak areas; peak efficiencies and *P/T* ratios; cascade summing correction; etc.

The LMN personnel at the IPEN have developed their own codes for aquisition and data analysis and applied them for routine use and research [e.g. 1–4]. Following this purpose, it was decided to create a new software package called *k0-IPEN* for mass fraction determination of irradiated samples. This package includes a methodology that unifies all the previous codes of the LMN in a

single process. In addition, the LMN expertise in covariance analysis, as demonstrated in previous papers [3–5], was fully incorporated in this new code. The advantage of such a code is to provide autonomy for the IPEN, allowing for parameter update and adjustments, and assuring independence from external software. Another advantage is to use it as an option for comparing results with well-known softwares, such as HyperLab [6], Kaywin [7] or k0-IAEA [8]. As a matter of fact, this was the motivation for an international comparison recently sponsored by the IAEA [9], in which the code k0-IPEN has participated. During this comparison it was shown that even well known softwares may show differences in the results, depending on the input parameters, and needing intervention from the developer in order to achieve the correct results. This comparison was successfully used for helping to develop the code. As suggested during the comparison, an ideal code should do all tasks related to $k_0$-NAA ($k_0$—Neutron Activation Analysis) in a fully automatic way. This was achieved by k0-IPEN, except in a few aspects, as described in the next sections. A significant feature of this code was the use of covariance matrix methodology to determine accurately the uncertainties in the parameters involved, for all steps of the mass fraction determination. This is not usually observed in other software packages found in the literature. The code was written in

✉ Mauro Da Silva Dias
  msdias@ipen.br

[1] Research Reactor Center (CERPq), Instituto de Pesquisas Energéticas E Nucleares (IPEN-CNEN/SP), Av. Prof. Lineu Prestes. 2242, São Paulo 05508-000, Brazil

Fortran language and does not have a graphical interface yet, therefore it is not intended to be used by a technician. However, once the user gets familiar with the procedure, he can achieve good results in a relatively short time.

## Methodology

### Block diagram of the code

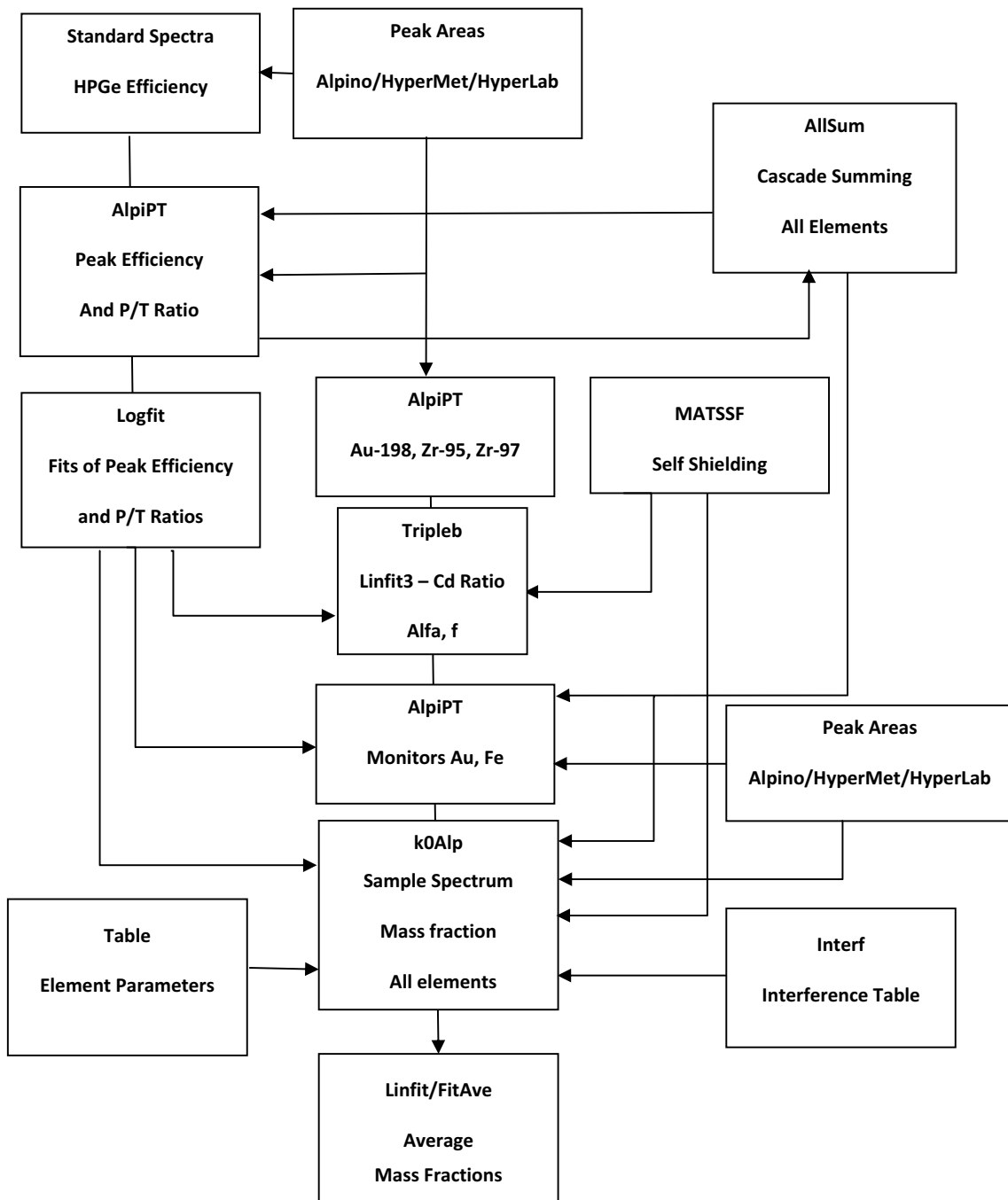A simplified block diagram of code k0-IPEN is shown in Fig. 1.



**Fig. 1** Simplified block diagram of code k0-IPEN

## Peak area determination

For the cases of well separated peaks, such as found in standard sources, the code may use routine Alpino [10] which is imbedded in the package. This routine performs simple integration of counts around the peak, in a region between $-1.5 \times$ FWHM and $+1.5 \times$ FWHM, and the average of two background regions, defined respectively between $-2.5 \times$ FWHM and $+1.5 \times$ FWHM and $+1.5 \times$ FWHM and $+2.5 \times$ FWHM. However, it is not able to resolve overlapping peaks. It is useful for calculating the net areas of well separated peaks and the detection limit for a given nuclide, which requires reading of counts directly from the measured spectrum. For the cases of overlapping peaks, the net peak areas can be read from the peak list generated by other codes, such as Hypermet [11] or HyperLab [6]. These peak areas are very close to the ones calculated by Alpino [10], when the peaks are well separated.

## Efficiency determination

When the source activity is known, such as the case of standard sources, code Alpino can calculate the detection efficiency, together with all partial uncertainties involved, namely: decay, dead time, self-attenuation, etc. An extended version of Alpino [10], called AlpiPT, also incorporates the calculation of the *P/T* ratio and corresponding uncertainty.

The efficiency must be corrected for cascade summing which in turn depends on the peak efficiency and *P/T* ratio. Therefore, the final efficiency is obtained after two steps: (a) calculation of peak efficiency and *P/T* ratio, without cascade summing correction; (b) application of cascade summing correction to the previous peak efficiency.

The cascade summing correction is calculated automatically by routine Allsum, applying the Semkow matrix formalism [12]. Since the cascade summing correction for a given energy of a radionuclide requires the values of peak efficiencies and *P/T* ratios for several other energies present in the decay scheme, an interpolation procedure becomes necessary. This interpolation is accomplished by a routine called Logfit [13], which performs a polynomial least square fit between the efficiency and gamma-ray energy, in log–log scale. This code considers all correlations between the partial uncertainties present in the calculation.

After application of the cascade summing correction to the preliminary experimental efficiencies, a new polynomial fitting in log–log scale is performed in order to obtain the final efficiency and *P/T* ratio curves.

## Monte Carlo modelling for efficiency transfer

At a reference large distance, the efficiency can be obtained accurately with experimental standard source data. In the present case, this distance was 202 mm and a total of 49 experimental points were used. However, other distances closer to the detector are necessary for measuring the samples, and the efficiency for these other geometries must be determined. At smaller distances, the cascade summing correction becomes very large for radionuclides with several gamma transitions, such as $^{152}$Eu and $^{133}$Ba, and the high uncertainty in the calibration prevents an acceptable result. At these distances, the experimental points can only be obtained by monoenergetic standard sources, which are available only in a limited number. This difficulty has been circumvented in other codes by using procedures to perform this efficiency transfer based on analytical tools or Monte Carlo methods [e.g. 14, 15].

In the present approach, this efficiency transfer was performed applying the Monte Carlo code MCNP6 [16]. An example of the geometry is shown in Fig. 2, as depicted by code VISED, which is incorporated in the MCNP package. In this figure, the source corresponds to a sediment encapsulated inside a cylindrical polyethylene container, in
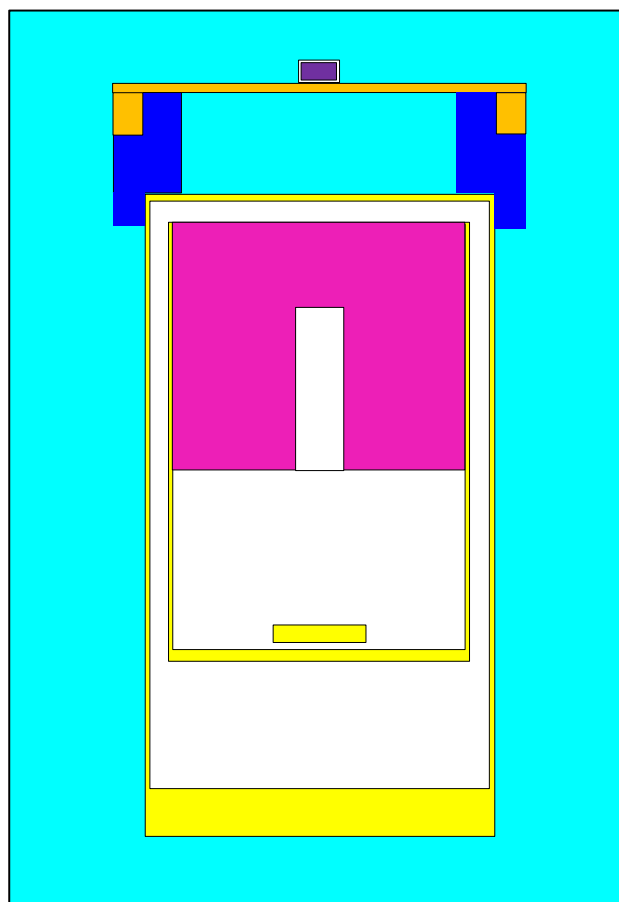


**Fig. 2** Monte Carlo modelling for MCNP6, as depicted by code VISED. The HPGe is shown in pink, the aluminium components in yellow, the source holder in blue and orange, and the sediment sample in violet

accordance to the international comparison measurement condition. This model was easily changed to a standard source geometry, in order to compare with the experimental calibration points. In this way, it was also possible to calculate the correction factor for source dimensions and materials. The geometrical parameters, such as source-crystal distance and detector hole dimensions were optimized by comparing the calculated efficiency results to the few experimental data points, available for each geometry, obtained with monoenergetic radionuclides. Once the geometry was established, MCNP6 was set to run for 34 gamma-ray energies from 50 to 3000 keV. Finally, polynomial fits were performed for interpolating between the calculated values, for peak efficiencies and $P/T$ ratios. An example of this polynomial fit is shown in Table 1 ($c_i$ coefficients) obtained at 22 mm source to detector distance. Since the experimental points were scarce (only eight points, from 59 to 1115 keV) the extrapolation to high energies (above 1500 keV) was not considered satisfactory, because it showed a discrepancy larger than 4%. Improvements in the modelling are necessary to overcome this problem.

## $\alpha$ and $f$ determination

These parameters were evaluated prior to the element mass fraction determination, as indicated in Fig. 1. Two methods were included in k0-IPEN for this purpose: (1) the Triple Bare method, which uses $^{198}$Au, $^{95}$Zr and $^{97}$Zr, performed by routine *Tripleb*, and (2) the Cd Ratio method, which may use several targets for a wide range of resonance energies, for instance: $^{198}$Au, $^{95}$Zr, $^{97}$Zr, $^{59}$Fe and $^{65}$Zn. These methods are well described by De Corte [17].

The Cd ratio method requires a linear least square fit in order to obtain the parameters. For this purpose, code Linfit [18] was included in the package and embedded in the general code. This code considers all correlations between the partial uncertainties present in the calculation.

## Specific count rate $A_{SP}$.

The next step is the calculation of the *Specific Count Rate* $A_{SP}$, performed by routine *k0Alp*. This parameter is defined as [17, 19]:

$$A_{sp} = \frac{N_p/t_m}{SDCw} \tag{1}$$

where:

$N_p$ is the net peak area,
$t_m$ the measurement time (s),
$w$ the mass of the element (g).

**Table 1** Parameters associated to the efficiency curves, $\alpha$ and $f$ average values and neutron fluxes

| Parameter | Value | Unc | Covariance matrix | | | | |
|---|---|---|---|---|---|---|---|
| $a_0$ | −1.1232E+02 | 1.9E+00 | 3.4441E+00 | | | | |
| $a_1$ | 6.8196E+01 | 1.3E+00 | −2.4207E+00 | 1.7054E+00 | | | |
| $a_2$ | −1.6031E+01 | 3.4E−01 | 6.2763E−01 | −4.4321E−01 | 1.1544E−01 | | |
| $a_3$ | 1.6471E+00 | 3.9E−02 | −7.1210E−02 | 5.0397E−02 | −1.3156E−02 | 1.5026E−03 | |
| $a_4$ | −6.3143E−02 | 1.6E−03 | 2.9863E−03 | −2.1179E−03 | 5.5406E−04 | −6.3411E−05 | 2.6816E−06 |
| $\chi^2/v$ | 1.19 | | | | | | |
| $b_0$ | −9.8961E+00 | 3.3E+00 | 1.0701E+01 | | | | |
| $b_1$ | 1.4962E+00 | 8.9E−01 | −2.9124E+00 | 7.9281E−01 | | | |
| $b_2$ | −1.5747E−01 | 6.1E−02 | 1.9794E−01 | −5.3895E−02 | 3.6646E−03 | | |
| $\chi^2/v$ | 0.78 | | | | | | |
| $c_0$ | −3.094E+02 | 1.3E+01 | 1.60E+02 | | | | |
| $c_1$ | 2.380E+02 | 1.1E+01 | −1.41E+02 | 1.24E+02 | | | |
| $c_2$ | −7.280E+01 | 3.9E+00 | 4.89E+01 | −4.32E+01 | 1.51E+01 | | |
| $c_3$ | 1.101E+01 | 6.7E−01 | −8.37E+00 | 7.41E+00 | −2.58E+00 | 4.44E−01 | |
| $c_4$ | −8.266E−01 | 5.7E−02 | 7.07E−01 | −6.26E−01 | 2.19E−01 | −3.76E−02 | 3.20E−03 |
| $c_5$ | 2.464E−02 | 1.9E−03 | −2.36E−02 | 2.09E−02 | −7.31E−03 | 1.26E−03 | −1.07E−04 | 3.59E−06 |
| $\chi^2/v$ | 1.24 | | | | | | |
| $f$ | 2.91E+01 | 1.3E+00 | | | | | |
| $\alpha$ | −9.11E−03 | 4.3E−03 | | | | | |
| $\phi$th (m$^{-2}$ s$^{-1}$) | 1.09E+16 | 1.5E+14 | | | | | |
| $\phi$epi (m$^{-2}$ s$^{-1}$) | 3.76E+14 | 1.7E+13 | | | | | |
| $\phi$fast (m$^{-2}$ s$^{-1}$) | 1.41E+15 | 1.9E+14 | | | | | |

In Eq. (1), the saturation factor $S$, the decay factor $D$ and the counting factor $C$ are well described in the literature [17, 19].

The net peak areas can be determined by codes Alpino [10], Hypermet [11] or HyperLab [6], but usually the latter is chosen because it can be used for overlapping peaks with high accuracy.

## Mass fraction of the element

The analyte mass fraction is calculated by routine k0Alp, and is given by [17, 19]:

$$\rho_a = \rho_c \frac{A_{sp,a}}{A_{sp,c}} \frac{k_{0,c}}{k_{0,a}} \frac{c_c \varepsilon_c}{c_a \varepsilon_a} \frac{\phi_{s,c}\left(fg_{th,c} + g_{epi,c}Q_{0,c}(\alpha)\right)}{\phi_{s,a}\left(fg_{th,a} + g_{epi,a}Q_{0,a}(\alpha)\right)} \quad (2)$$

where:

Indexes $a$ and $c$ correspond to analyte and comparator, respectively,

$\rho$ is the mass fraction,

$c$ the cascade summing correction,

$\varepsilon$ the detection peak efficiency,

$\Phi_s$ the thermal neutron fluence rate (m$^{-2}$ s$^{-1}$),

$f$ the thermal/epithermal flux ratio $f = \Phi_s/\Phi_{epi}$,

$g_{th}$ and $g_{epi}$ are the thermal and epithermal self-shielding corrections, respectively, and.

$\alpha$ the deviation from the ideal $1/E$ epithermal neutron spectrum,

The dependence of $Q_0(\alpha)$ on $\alpha$ and the effective resonance energy $E_r$ is given by [17, 19]:

$$Q_0(\alpha) = \frac{Q_0(0) - 0.429}{E_r^\alpha} + \frac{0.429}{(2\alpha + 1)E_{Cd}^\alpha} \quad (3)$$

where:

$Q_0(0) = I_0/\sigma_0$,

$\sigma_0$ the thermal capture cross section (m$^2$), and.

$I_0$ the resonance integral (m$^2$).

Alternatively, using Au as comparator, the mass fraction can be given by:

$$\rho_a = \frac{A_{sp,a}}{F_c} \frac{1}{k_{0,a}} \frac{1}{c_a \varepsilon_a} \frac{\phi_{s,c}}{\phi_{s,a}} \frac{1}{\left(fg_{th,a} + g_{epi,a}Q_{0,a}(\alpha)\right)} \quad (4)$$

where $F_c$ is called *comparator factor*, which depends only on comparator parameters given by:

$$F_c = \left[\frac{\rho_c}{A_{sp,c}} \frac{k_{0,c}}{1} c_c \varepsilon_c \left(fg_{th,c} + g_{epi,c}Q_{0,c}(\alpha)\right)\right]^{-1} \quad (5)$$

The thermal flux $\phi_{s,c}$ can be calculated from $F_c$ as described in reference [19].

The necessary parameters associated with the element to be analysed, such as: $k_0$, $Q_0$, half-life, gamma-ray yield, etc., were obtained from the $k_0$-Database [20] and from the DDEP_WG recommended decay data [21].

## Interference correction

The presence of undesirable counts inside or very close to a given gamma-ray peak must be considered, in order to obtain the correct mass concentration. For this purpose, a standard interference table was used [22] and imbedded in routine k0Alp. For each measured peak, this table was scanned, and the interference correction was calculated automatically by the following expression [19]:

$$N_{p,x} = N_{p,x+y} - N_{p,z}R_{int} \quad (6)$$

where:

$N$ is the net peak area,

indexes $x$, y and $z$ correspond respectively to: nuclide of interest; interfering nuclide at an energy close to the nuclide of interest (causing the interference); interfering nuclide at another energy, free from interferences.

The factor $R_{int}$ is given by

$$R_{int} = \frac{\gamma_y \cdot \varepsilon_{p,y} \cdot c(y)}{\gamma_z \cdot \varepsilon_{p,z} \cdot c(z)} \quad (7)$$

where:

$\gamma$ is the gamma yield,

$\varepsilon$ is the detection peak efficiency, and.

$c$ is the cascade summing correction.

The energy separation between the nuclides $x$ and $y$ can be selected as desired. Usually it was around 0.5 keV, when the peak area was taken from HyperLab [6] peak-list.

## Average value of mass fraction

The last step is the calculation of the mass fraction averaged value and its corresponding uncertainty. This is performed by routine FitAve in connection with routine Linfit [18]. At this point, the user intervention is necessary to select the mass fraction results that should be included in the average, from those that should be discarded, because they increase the final uncertainty.

## Detection limit

The detection limit expression was taken from the IAEA recomendation [Ref. 23, p. 21]. The calculation considers the counts from the original spectrum, in a region near the peak of interest. The *Paired Measurement* methodology was applied, using the following equation:

$$ky = \frac{\left[k + \sqrt{8.n_b}\right]}{\left[1 - \left(k.u_{rel}(y)\right)^2\right]} \qquad (8)$$

where:

$k$ is the coverage factor,

$n_b$ is the background counts,

$u_{rel}(y)$ is the relative uncertainty of $y$ and.

$y$ is the value of the conversion function, including the measurement time.

## Uncertainty calculation

The overall uncertainty in the mass fraction was obtained by the propagation law [24, 25], considering all correlations between the parameters. The same procedure was followed by the fitting codes Logfit [13] and Linfit [18]. The covariance matrix associated with the efficiency curve coefficients was inserted in code k0Alp and propagated together with the other parameters. In the case of the Triple Bare method, since it uses an implicit equation, it was decided to use the Monte Carlo method for the propagation. A normal distribution was applied to each partial uncertainty and several runs were performed changing randomly the uncertainties around the normal distributions. The final values of the parameters $\alpha$ and $f$ were obtained as the average from all runs with corresponding uncertainties. The mass fractions for a given element, obtained from different irradiation and/or measurement condition, were averaged applying code Linfit [18] and considering all correlations and using covariance matrix methodology.

## Results

The data presented in this section are part of the IPEN results submitted to *The 2021 IAEA software intercomparison for $k_0$-INAA*. A full description of the experiment and analysis are described in the references [9, 26]. Here a brief review of the results is shown, only for illustration of the use of the k0-IPEN software package. A screen shot showing a small sample of the output file is shown in Fig. 3. All partial uncertainties are given.

**Fig. 3** Screen shot showing a small sample of the output file

```
*************************************************************************************** *

GENERAL PARAMETERS OF IRRADIATION AND MEASUREMENT

Sample 4 Spectrum R1973F-6.chn 200 mm - Monitor 200 mm

FLUX PARAMETERS

FTH (M-2.S-1)   SFTH(%)  FEPI (M-2.S-1)  SFEPI(%)  FFAST (M-2.S-1)  SFFAST(%)
1.136E+16       1.84     3.824E+14       3.02      1.410E+15        13.55

F0          SF0(A)    Alfa0     SAL0(A)   IR (H)    STIR(%)   FGRAD     SFGRAD(%)
2.970E+01   1.30E+00  9.400E-03 1.01E-02  1.200E+01 8.30E-03  9.800E-01 3.00E-01

FCAU1       SFCAU1(%)   FCAU2      SFCAU2(%)
1.1030E+04  3.02        1.1030E+04 2.92

MONITOR PARAMETERS

MONITOR    T12M(D)    ST12M(%)  K0M       SK0M (%)  Q0M       SQ0M(%)  Q0MA      SQ0MA(%)
Au Au198   2.6943E+00 .00       1.0000E+00 .00      1.5700E+01 1.80    1.5448E+01 1.88

ERM        SERM(%)  GTHM     SGTHM(%)  GEPIM    SGEPIM(%)  MASM(g)   SMASM(%)  MASMAU(g)  SMASMAU(%)
5.650E+00  7.10     9.994E-01 .01      9.981E-01 .04       9.300E-03 .20       9.328E-06  .20

TM LIVE(S) TM REAL(S)  T BG(S)    MEAS DATE  MEAS TIME  REF DATE   REF TIME
 450.00     459.06     45000.00   5/ 9/2018  6:30:47    30/ 8/2018 16:53: 0

EGMON      AREAM     SAREAM(%)   AREAMC    SAREAMC(%)  FDEADM   SFDEADM   FATM      SFATM
411.80     105409.0  .31         107531.2  .31         1.02013  .00       1.00130   .03

EGMON      FSUMM     SFSUMM(%)  ASPM     SASPM(%)  ASPM2    SASPM2(%)  ACTIVM    SACTIVM(%)
411.80     9.999E-01 .00        8.646E+08 .86      8.721E+08 .37       6.275E+07 .55

EGMON      EFM       SEFM(%)  EFMCOR    SEFMCOR(%)  FSATM     SFSATM(%)  FGM      SFGM(%)  SDCM      SSDCM(%)
411.80     1.753E-03 .35      1.769E-03 .46         1.207E-01 .01        9.900E-01 .30     2.880E-02 .01
```

## Efficiency curve

Figure 4 shows the peak efficiency curve obtained with 49 experimental points, at the reference position, corresponding to a distance of 202 mm from a point source to the detector cap [9, 26]. Here the energy range was from 53 to 2447 keV. The net peak areas were obtained by code HyperLab [6]. The continuous line corresponds to the polynomial fitting. Figure 5 shows the residuals between the experimental points and a 4th degree polynomial fitting in log–log scale, applying routine Logfit [13]. The points are in overall agreement with the fitting, showing no special bias. The polynomial coefficients and the corresponding covariance matrix are shown in Table 1 ($a_i$ coefficients). The resulting reduced chi-square was 1.19 indicating a satisfactory fit. Table 1 also shows the fitting coefficients for 20 experimental points from 1112 to 2447 keV, applying a 2nd degree polynomial ($b_i$ coefficients). This latter curve was designed to cover energies up to 3000 keV. In
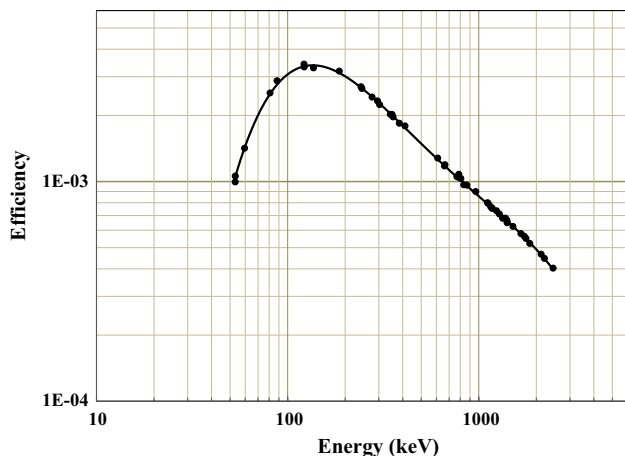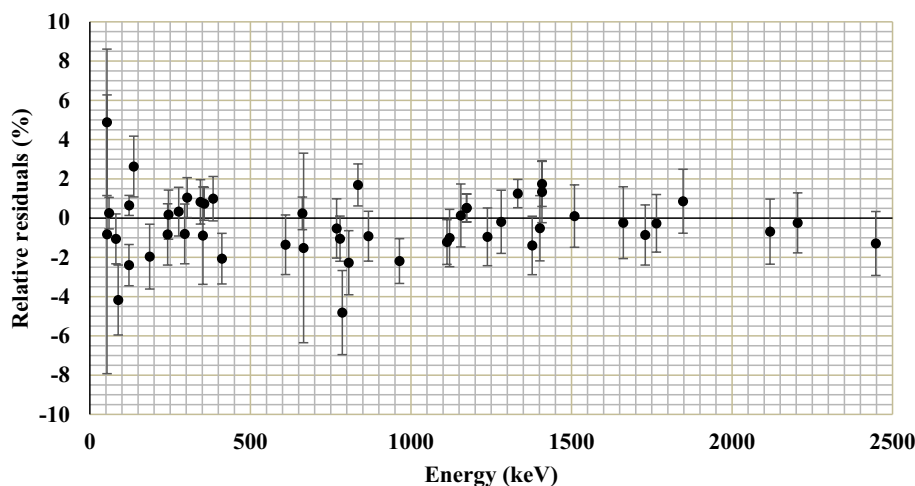
this case, the reduced chi-square was 0.78, which can be considered satisfactory. This table also includes the fitting parameters ($c_i$ coefficients) for 34 calculated points at 22 mm source to detector distance. The reduced chi-square was 1.24, which can be considered adequate.

## Flux parameters

Table 1 also shows the values of $\alpha$ and $f$ from the Triple Bare method, and their corresponding uncertainties. The Cd ratio method was not used in this case because it increased the uncertainty. The thermal, epithermal, and fast fluxes are also given.

## Mass fractions

Table 2 shows the results for mass fractions of some elements contained in the irradiated sample and the comparison with certified values. The performance of the results with respect to certified values was tested by calculating the $E_n$ score, defined by the following equation [23, 27]:

$$E_n = \frac{X_{\text{lab}} - X_{\text{ref}}}{\sqrt{U_{\text{lab}}^2 + U_{\text{ref}}^2}} \tag{9}$$

where $U_{\text{lab}}$ and $U_{\text{ref}}$ are the expanded uncertainties ($k = 2$) of the experimental result and the assigned value of CRM (Certified Reference Material), respectively. The agreement can be considered satisfactory since $E_n$ is lower than 1 in all cases. The bias, i.e., the deviation with respect to the certified values are also presented, for comparison.

Mass fractions ($X_{\text{CRM}}$, $X_{\text{lab}}$) are expressed in mg/kg and expanded uncertainties ($U_{\text{ref}}$, $U_{\text{lab}}$) with a coverage factor $k = 2$.



**Fig. 4** Peak efficiency curve at 202 mm, source to detector distance. The continuous line corresponds to the polynomial fitting

**Fig. 5** Residuals between experimental efficiencies at 202 mm and the polynomial fitting

**Table 2** Mass fractions of some elements contained in the irradiated sample (IRMM BCR–320R)

| Element | Assigned value | | | k0-IPEN | | | | | $E_n$ | Bias (%) |
|---|---|---|---|---|---|---|---|---|---|---|
| | $X_{CRM}$ | ± | $U_{ref}$ | $U_{ref}$ (%) | $X_{lab}$ | ± | $U_{lab}$ | $U_{lab}$ (%) | | |
| As | 21.7 | ± | 2.0 | 9.2 | 21.8 | ± | 3.3 | 14.9 | 0.03 | 0.5 |
| Co | 9.7 | ± | 0.6 | 6.2 | 10.1 | ± | 0.5 | 4.9 | 0.52 | 4.2 |
| Cr | 59 | ± | 4 | 6.8 | 60 | ± | 4 | 6.6 | 0.26 | 2.4 |
| Fe | 25,700 | ± | 1,300 | 5.1 | 25,726 | ± | 1,281 | 5.0 | 0.01 | 0.1 |
| Hg | 0.85 | ± | 0.09 | 11 | 0.85 | ± | 0.12 | 13.9 | −0.01 | −0.1 |
| Mn | 910 | ± | 50 | 5.5 | 907 | ± | 56 | 6.2 | −0.04 | −0.4 |
| Sc | 5.2 | ± | 0.4 | 7.7 | 5.4 | ± | 0.3 | 6.2 | 0.44 | 4.4 |
| Th | 5.3 | ± | 0.4 | 7.5 | 5.7 | ± | 0.3 | 4.8 | 0.76 | 6.9 |
| U | 1.56 | ± | 0.20 | 13 | 1.56 | ± | 0.11 | 7.2 | −0.01 | −0.1 |
| V | 46.5 | ± | 2.8 | 6.0 | 45.4 | ± | 4.4 | 9.6 | −0.22 | −2.5 |
| Zn | 319 | ± | 20 | 6.3 | 329 | ± | 19 | 5.9 | 0.35 | 3.1 |

## Conclusions

The Nuclear Metrology Laboratory (LMN—Laboratório de Metrologia Nuclear) of the Nuclear and Energy Research Institute (IPEN—Instituto de Pesquisas Energéticas e Nucleares) in São Paulo, Brazil, developed a software package for Neutron Activation Analysis (NAA) called k0-IPEN. This software runs automatically, following all steps necessary to obtain the mass fractions of the elements involved. Covariance matrix methodology was used to determine accurately the uncertainties in the parameters involved, for all steps of the process. With this software the LMN has participated in an international comparison sponsored by the IAEA, showing good results [9, 26]. However, improvements are foreseen, such as automatic calculation of self-shielding factors, inclusion of interference from threshold reactions and more accuracy in the Monte Carlo modelling, mainly in the high gamma-ray energy region, and short source to detector distances. In addition, a graphical interface is planned to be included, in order to make it easier to input the necessary data.

## Declarations

**Conflict of interest** This paper does not incur potential conflicts of interest.

**Human or animal participants** No human test subjects or animals played a part.

## References

1. Ferreira FA Jr, Maidana NL, Vanin VR, Dias MS, Koskinas MF, López-Pino N (2012) $^{41}$K(n, γ)$^{42}$K thermal and resonance integral cross section measurements. Radiochim Acta 100(12):871–878. https://doi.org/10.1524/ract.2012.1985
2. Maidana NL, Dias MS, Koskinas MF (1998) Measurement of the thermal neutron capture cross section of Cs-137. Radiochim Acta 83:117. https://doi.org/10.1524/ract.1998.83.3.117
3. Dias MS, Cardoso V, Koskinas MF, Yamazaki IM, Semmler R, Moralles M, Zahn GS, Genezini FA, de Menezes MO, Figueiredo AMG (2011) Measurements of $k_0$ and $Q_0$ values for $^{64}$Zn(n, γ)$^{65}$Zn and $^{68}$Zn(n, γ)$^{69m}$Zn reactions with covariance analysis. Appl Radiat Isot 69:960–964. https://doi.org/10.1016/j.apradiso.2011.03.026
4. Barros LF, Dias MS, Koskinas MF (2022) Experimental determination of $k_0$ and $Q_0$ values for $^{121}$Sb, $^{123}$Sb and $^{130}$Ba targets applying covariance analysis. Appl Radiat Isot 184:1–7. https://doi.org/10.1016/j.apradiso.2022.110122
5. Barros LF, Ribeiro RV, Dias MS, Moralles M, Semmler R, Yamazaki IM, Koskinas MF (2019) Determination of $k_0$ and $Q_0$ for $^{74}$Se, $^{113}$In, $^{186}$W and $^{191}$Ir targets applying covariance analysis. Appl Radiat Isot 154:108846. https://doi.org/10.1016/j.apradiso.2019.108846
6. HyperLab (2014) Quick start guide for main model. HyperLabs Software, Budapest, Hungary
7. Kayzero for Windows—KayWin® (2005), User's manual for reactor neutron activation analysis (NAA) using the $k_0$ Standardization Method, Version 2.
8. Rossbach M, Blaauw M, Bacchi MA. Lin X (2007) The k0-IAEA program. J Radioanal Nuclear Chem 274(3):657–662. https://doi.org/10.1007/s10967-007-7104-4
9. IAEA TECDOC Series (2022) The 2021 intercomparison of software for k0-INAA. Vienna (to be published)
10. Dias M S, Alpino V.1 (2001) User manual. internal report. Nuclear Metrology Laboratory. IPEN-CNEN/SP, São Paulo, Brazil
11. Hypermet (2008) Institute of Isotopes, Budapest, https://www.iki.kfki.hu/nuclear/hypc/index_en.shtml. Accessed 07 Jul 2022

12. Semkow TM, Mehmood G, Parekh PP, Virgil M (1990) Coincidence summing in gamma-ray spectroscopy. Nucl Instrum Methods Phys Res Sect A Accel Spectrom Detect Assoc Equip 290:437–444. https://doi.org/10.1016/0168-9002(90)90561-J

13. Dias MS, Moreira DS (2005) LOGFIT V.1 -Program for Polynomial Fitting with Covariance. User Manual. Internal Report. Nuclear Metrology Laboratory. IPENCNEN/SP, São Paulo, Brazil

14. Vidmar T (2005) EFFTRAN—A Monte Carlo efficiency transfer code for gamma-ray spectrometry. Nucl Instrum Meth Phys Res Sect A 550:603–608. https://doi.org/10.1016/j.nima.2005.05.055.

15. Pylypchynets I, Lengyel A, Parlag O et al (2019) Empirical formula for the HPGe-detector efficiency dependence on energy and distance. J Radioanal Nucl Chem 319:1315–1319. https://doi.org/10.1007/s10967-019-06426-8

16. Goorley JT, James, MR, Booth TE, Brown FB, Bull JS, Cox LJ, Durkee JW Jr, Elson JS, Fensin ML, Forster RA III, Hendricks JS, Hughes HG III, Johns RC, Russell C (2013) Initial MCNP6 Release Overview—MCNP6 version 1.0-LA-UR-13-22934

17. De Corte F (1987) The k0-standardization method—a move to the optimization of neutron activation analysis, habil. Thesis, INW, Gent, Belgium

18. Dias M S (2001), LINFIT V.1—Program for the least squares method with covariance analysis. User Manual. Internal Report. Nuclear Metrology Laboratory, IPEN-CNEN/SP, São Paulo, Brazil

19. VADE MECUM for k0-Users http://www.kayzero.com/VADE%20MECUM%20FOR%20k0%20KayWin%20V3.pdf, Accessed 15 july 2021

20. Jaćimović R (2020), k0 Database [WWW Document] http://www.kayzero.co/k0naa/k0naaorg/Nuclear_Data_SC/Entries/2020/8/24_Update_of_k0-database_I-128.html, Accessed 15 july 2021

21. Decay Data Evaluation Project. Laboratoire National Henri Becquerel. http://www.lnhb.fr/ddep_wg/, Accessed 15 july 2021

22. Blaauw M (1996) The k0-Consistent IRI Gamma-ray Catalogue For INAA, p. 75. Interfacultair Reactor Instituut van de Technische Universiteit Delft

23. Determination and Interpretation of Characteristic Limits for Radioactivity Measurements. Decision Threshold, Detection Limit and Limits of the Confidence Interval., 2017. IAEA Analytical Quality in Nuclear Applications Series No. 48. IAEA, Vienna

24. Smith D L (1991) Probability, Statistics and Data Uncertainties in Nuclear Science and Technology. Illinois-ANS

25. BIPM (2008) Guide to the expression of uncertainty in measurement, JCGM 100:2008 (GUM 1995 with minor corrections)

26. Blaauw M, D'Agostino G, Di Luzio M, Dung, H M, Jacimovic R, Dias M S, Semmler R, Van Sluijs R, Barradas N P (2022) The 2021 IAEA software intercomparison for k0-INAA. Available online: https://doi.org/10.1007/s10967-022-08626-1

27. International Standard ISO 13528 (2005) Statistical methods for use in proficiency testing by interlaboratory comparisons. ISO, Geneva